REVISION 2

Oriented aggregation as a crystal growth mechanism in natural environments (the sepiolite-palygorskite polysomatic series)

Emilia García-Romero[1, 2], Mercedes Suárez[3].

1 Departamento de Cristalografía y Mineralogía, Universidad Complutense de Madrid, 28040 Madrid, Spain.

2 Instituto de Geociencias (UCM-CSIC), 28040 Madrid, Spain.

3 Departamento de Geología. Universidad de Salamanca, Patio de Escuelas 1, 37008 Salamanca, Spain.

Abstract.

A detailed microscopic study of sepiolite and palygorskite natural samples reveals that, independently of the fiber length, they all are composed of other minor width fibers until the minor units or the true crystals. They are prismatic crystals elongated along [001] with rhombus-like morphology in cross-section, designated laths. Although their length can vary greatly, their width is always nanometric (~10-30 nm). The laths are grouped in a crystallographic

arrangement, sharing edges or faces forming rods. Several rods, parallel to the c-axis of the fiber, form bundles. The laths are the smallest stable nucleated crystals. After the nucleation, the process of growth continues via a non-classic crystal growth mechanism, (aggregation of the nanolaths). Subsequently, the aggregated sepiolite and palygorskite natural crystals can continue growing, along the c-axis at the expense of the diffusion of molecular scale species throughout the solution. The morphology of the faces is controlled by the highly different attachment energy of the faces.

Keywords: sepiolite, palygorskite, polysomatic series, non-classic nucleation, oriented aggregation, mesocrystals, electron microscopy, crystal growth.

Introduction

Research examining the properties and behaviors of the fibrous clay minerals sepiolite and palygorskite is important to both materials and earth sciences. Sepiolite and palygorskite have played and continue to play very important roles in a huge number of industrial processes (Álvarez 1984; Jones and Galán 1991; Murray 1999; Álvarez et al. 2011). Humanity has used sepiolite and palygorskite since ancient times in pharmaceutical products and cosmetics (Cornejo 1990; Carretero2002; López-Galindo and Viseras 2004; Carretero et al. 2006) due to their colloidal size and crystalline structure. Hybrid nanomaterials based on sepiolite and palygorskite have been known for several centuries, such as Maya blue pigment (Sánchez del Río et al. 2011). In addition to their traditional applications, new uses for these minerals have been developed in recent years, such as their adaptation as vehicles for systems with modified release of active agents (López-Galindo et al. 2011).

Besides these minerals' classic uses as ad- and absorbents, as rheological additives or in filtration and sieving processes, they are widely used as nanofillers in the preparation of polymer/clay nanocomposites or as nanoadditives (Billotti et al. 2008; Ruiz-Hitzky et al. 2011) or organomodified nanoclays (Ruiz-Hitzkyand Van Meerbeek 2006), all of which have attracted considerable interest in recent years. Sepiolite and palygorskite behave similarly to many clay minerals in their ability to assemble organic species and produce organic–inorganic hybrid materials (Ruiz-Hitzky et al. 2004). Organic species can interact with sepiolite mainly at the external surface and in some cases also within the internal surface by penetration into its structural tunnels. In fact, sepiolite and palygorskite act as molecular sieves that discriminate the adsorption of species by their molecular size. Bio-nanohybrid materials are an emerging class of organic–inorganic hybrids that result from the assembly of molecular or polymeric species of biological origin on inorganic substrates through interactions at the nanometric scale (Ruiz-Hitzky et al. 2011). In the incoming era of nanotechnology, sepiolite and palygorskite are very promising for advanced applications as diverse as nanofillers in polymer–clay nanocomposites, support of nanoparticles for sensor devices and high-performing catalysts or even building clay-biological interfaces for tissue engineering, new adjuvants for vaccines and bioreactor devices.

The surface properties of sepiolite and palygorskite and their ability to interact with many compounds to form nanostructured materials is related not only to their nanosize but also to the presence of tunnels, channels and different types of water molecules in the structure, along with the hierarchical distribution of pores and the presence of silanol groups (Si-OH) on the external surface. Sepiolite and palygorskite are the end-members of a continuous polysomatic series (Suárez and García-Romero, 2013). Both minerals are modulated fibrous phyllosilicates 2:1, formed by continuous sheets of

63 tetrahedral silica with periodically inverted apical oxygen. This periodical inversion produces
64 discontinuous octahedral sheets in the [010] direction, resulting in ribbons or polysomes along the
65 [001] direction. Each ribbon is two chains wide for palygorskite and three chains wide for sepiolite in
66 [010] (Figure1). The discontinuity of the octahedral sheet leads to the formation of the tunnels and
67 channels. Tunnels are present at the inner of the particle, among the polysomes, and form the internal
68 surface. Channels are open tunnels at the edge of the particle and form the external surface. Both
69 tunnels and channels run parallel to the c-axis of the crystal and are accessible or partially accessible to
70 different molecules. These structures induce the fibrous morphology of sepiolite and palygorskite and
71 are responsible for the high values of the specific surface areas of the two minerals. However, despite
72 having the same fibrous microtexture, it is remarkable that natural samples of different deposits display
73 different specific textural features when studied by electron microscopy (both scanning and
74 transmission). The length and width of their fibers, curliness and textural porosity are notably different
75 (Suárez and García Romero 2012). These different textural features determine their properties and uses
76 and, are due to differences in the thermodynamic and kinetic conditions present during formation.
77
78 Currently, nonclassical crystallization models are used to complement classical crystal growth theory.
79 The term *Nonclassical crystallization* describes processes which involve parallel multiple nucleation
80 events that form nanoparticles that then form a superstructure (in stark contrast to a single nucleation
81 event forming a single crystal) and the self-assembly of preformed nanoparticles to an ordered
82 superstructure, which then can fuse to a single crystalline structure. Nonclassical crystallization
83 comprises oriented aggregation of nanoparticles and mesocrystals formation. It has been proposed as
84 growth mechanism for the fibrous minerals that involves a number of novel steps that have been
85 elucidated in several studies (Penn and Bandfield 1988, 1999; Penn 2004; Cölfen and Antonietti 2008),

which provide examples of synthetic materials and growth in the laboratory (e.g., metal oxides, selenides and sulfides) from initially homogeneous solutions. "Oriented aggregation is a special case of aggregation that provides an important route by which nanocrystals grow, defects are formed, and unique, often symmetry-defying, crystal morphologies are produced" (Pen 2004). The process is particularly relevant in nanocrystalline regimes with relatively high specific surface areas, where bonding between the particles allows the system to acquire a substantial amount of energy by eliminating two high-energy surfaces by crystallographic fusion as well as reducing entropy by the release of previously surface-attached molecules by crystallographic fusion (Banfield et al. 2000, Alivisatos 2000). In addition, it can lead to the production of anisotropic nanoparticles (elongated particles) (Cho et al. 2005; Yumono et al. 2010). Mesocrystals are a non-classical oriented aggregation consequence, built from crystallographically oriented nanoparticles. They are one intermediate steps in which the primary units can still be identified (Cölfen and Antonietti, 2005). To the best of our knowledge, in natural environments, there are only studies examining the aggregation of framboidal pyrite (Soliman and El Goresy 2012), in which the growth of individual aggregates of the microcrystals leads to the formation of combined micro-framboids and to the grouping of the several framboids of pyrite, but in these examples, unique single crystal morphologies are not produced. The terms aggregation and coalescence have sometimes also been used to explain the formation and stacking of mica layers (Nespolo 2001; Meunier 2005; Eberl et al. 2011). Recently, dolomite mesocrystals are cited by Leguey et al. (2010) describing the role of biomineralization in the origin of sepiolite and dolomite in Miocene sediments of the Madrid basin.

This work reports evidence of oriented aggregation in natural minerals, which is in contrast with the preponderance of previous research that provides examples of synthetic materials. The growth of

minerals of the sepiolite-palygorskite polysomatic series by oriented aggregation has not been previously reported. In addition, this work provides information concerning the precipitation of these minerals in aquatic environments, which contributes to the knowledge of the physico-chemical conditions present during the formation of numerous deposits of both minerals, certain of which have high economic importance.

Materials and methods

The study was conducted based on observations of a broad group of natural sepiolite (23) and palygorskite (25) samples. The samples came from different localities around the world and have different geological origins, from sedimentary to hydrothermal, including samples from the greatest deposits of sepiolite in the world, such as Vallecas-Vicálcaro, Cabañas de la Sagra and Mara in Spain, Polattli-Eiskisehir in Turkey and Nevada in the U.S.A., as well as deposits of palygorskite from the Yucatán in Mexico, Allou Kagne in Senegal, and Attapulgus in the U.S.A. The samples were previously studied with different objectives and their mineralogical, chemical and textural characterization can be found in Suárez et al. 1994; 2007; García-Romero et al. 2004; 2007; Suárez and García- Romero 2006-a -b; 2011; 2012; 2013; Sánchez del Río et al. 2009; 2011; Chryssikos et al. 2009; García-Romero and Suárez 2010; 2013-b; Statopoulou et al. 2011.

Scanning electron microscopy (SEM and FEG) and transmission electron microscopy (TEM) were used to study the textural features of both sepiolite and palygorskite fibers. SEM observations were performed using a JEOL JSM 6400 microscope, operating at 20 kV and equipped with a Link System energy dispersive X-ray microanalyser (EDX), and FEG observations were acquired with a JEOL

JSM-6330F (Field Emission Scanning Electron Microscope) operating at 10 kV, wd 15 mm and SEI. Prior to SEM-FEG examination, freshly fractured surfaces of representative samples were air-dried and coated with Au under vacuum. TEM observations were performed by depositing a drop of diluted suspension on a microscopic grid with cellulose acetate butyrate. The act of dispersion causes changes in the shape of the original particles. The milling not only separates the fibers but breaks a portion of them. This breakage has to be taken into account, and each image must be interpreted with the preparation method in mind. The main problem with clay minerals images is radiation damage. Their structure under the high-power density of the electron beam is quickly dehydrated and destroyed in a few seconds. To optimize the observations and avoid damage to samples, three different types of equipment with different acceleration voltages and different point-to-point resolutions were used: a JEOL 2000 FX microscope at an acceleration voltage of 200 kV, with 0.5 mm zeta-axis displacement and 0.31 nm point-to-point resolution; a JEOL JEM 2100 at an acceleration voltage of 200 kV, with a STEM detector, and 0.25 nm point-to-point resolution and a JEOL 3000 FX Field Emission microscope operated at an acceleration voltage of 200 kV with a 0.17 nm point-to-point resolution. In the case of higher acceleration voltage, only one exposure was acquired per view because after the exposure, the crystal became amorphous.

Results

Sepiolite and palygorskite, as clay minerals, are nanomaterials that can only be distinguished by electron microscopy. Sepiolite and palygorskite crystals are highly anisotropic, much longer than wide, and appear as fibrous materials under SEM-FEG. Murphy and Jana (2002) classified fibrous particles depending on the ratio of L/W (length to wide) into nanorods, for particles with L/W $\leq$ 20, and

nanowires for L/W > 20. After this classification most sepiolites and palygorskites are nanowires and only exceptionally can appear as nanorods. For these minerals García-Romero and Suárez (2013) proposed different typological classifications attending to several parameters and concluded that they can appear in four different types of fiber defined by the ratio L/W. The limits are <10, between 10 and 100, > 100 and, finally >>1000 for macroscopic fibers in which sections are nanometric but length can be centrimetric even. The length of the fibers varies greatly among the different deposits here studied, from less than 1 μm to centimeters with no gap. Most samples correspond to the intermediate types and only exceptionally very short or macroscopic fibers can be found. Detailed microscopic study reveals that independent of the fiber length, they all are composed of other minor-width fibers. When the magnification of the image is still larger, it is possible to verify that the minor fibers are also composed of other fibers of minor width that form minor structural units or crystals. The TEM and SEM-FEG observations indicate that the minerals are prismatic crystals elongated along the [001] direction (Figures 2 and 3). The minor width size units observed (minor crystals) have been designated laths (Figure 2A). They are the smallest stable crystals that can be observed using TEM and sometimes by SEM-FEG (only at more than 50000 magnification). Although the length of the fibers can vary greatly, the width of the laths is always nanometric (~10-30 nm), which is consistent with the observations of Martín Vivaldi and Robertson (1971). Generally, the laths are grouped in a crystallographic arrangement sharing edges or faces forming rods or bundles. A rod of sepiolite or palygorskite is formed by several crystals (laths) (Figures 2B, 3A, 3B), and several rods more or less parallel to the c-axis of the fiber form bundles (Figure 2D, 2E) (Singer, 1981; García-Romero and Suárez 2012, 2013-a 2013-b). Figure 2 shows TEM images of parallel laths of sepiolite and palygorskite with common faces or edges forming rods and bundles. The rods formed by laths joined parallel to the c-axis sharing the edges appear in Figure 2A, 2B. Figure 2C, 2D, 2D and 2F show

different images of bundles made by rods and laths grouped more or less parallel to the c-axis but without sharing faces or edges. The length of the bundles depends on the length of the individual laths or rods that form them, but usually, the bundle lengths are much longer than the individual laths (Figure 2E). In the same sample, laths can appear both aggregated and forming rods or can remain without aggregation (Figure 3C, 3D, 3E). The minor-size crystals or laths are ~10-30 nm wide as mentioned above. If the b parameter is 1.8 nm in palygorskite and 2.4 nm in sepiolite, the smallest stable crystals or laths (~10 nm) correspond to ~5.5 unit cells in the b-axis direction for palygorskite and ~4 for sepiolite. These findings indicate that, in the (001) section, the crystals have a size not much greater than during primary nucleation.

Discussion

The morphology and assembly of the laths to forming rods and bundles cannot easily be explained by conventional crystal growth models. Both the microstructure and the crystal shape point to a specific aggregate growth mechanism in the formation of sepiolite and palygorskite rods and also bundles (Penn 2004; Cölfen and Antonietti 2008). It is well-known that the first stage in the formation of crystals from aqueous solution is the nucleation (homogeneous or heterogeneous). The clusters that achieve critical nucleus size are stable and grow to form bigger crystals. According to the Gibbs–Thomson effect, small particles have a higher solubility than larger ones (Gibbs 1948). This is a direct consequence of the surface to volume ratio of the particles as the system minimizes its total surface free energy. In a saturated solution in equilibrium with crystals, a process of Ostwald ripening occurs (large crystals grow at the cost of smaller ones) (Ostwald 1896). The TEM study of the natural samples of sepiolite and palygorskite demonstrates that the smallest stable units formed in the starting material,

the nucleated crystals, are the laths. There are no smaller units because they are unstable and dissolve. After this first stage of nucleation, the process of growth continues mainly by aggregation, and the aggregation of the smaller laths is responsible for the formation of wider laths and rods.

Nanolaths aggregate to each other and grow via a non-classical crystal growth mechanism (Penn 2004; Cölfen and Antonietti 2008), which occurs via crystallographically oriented attachment, including rotation and oriented attachment of nanolaths. Oriented attachment occurs when particles join at specific dimensionally similar crystallographic surfaces. "When the interface of these growing laths and rods comes into contact these rotate to align with the crystallographic matching face of the substrate" (Grassmann et al. 2003). The aggregation of sepiolite and palygorskite crystals occurs parallel to the c-axis of the fibers by sharing faces (Figures 2B, 3A, 3B, 3E, 3F, 4 and 5). Grassmann et al. (2003) also affirmed that "the cluster aggregation is driven by reduction in surface free energy that is minimized if the clusters are in contact with a crystal face rather than with edges or vertices". The rods can be wider and much longer than the individual laths that form them because the laths attach to each other in different positions along the c-axis (Figure 2A). Both the laths and the rods can also aggregate more or less parallel to the c-axis but form small angles in bundles (Figure 2C, D, E). According to Pen (2004), "This growth mechanism involves the irreversible and crystallographically specific self-assembly of primary nanocrystals and results in the formation of new single crystals, twins and intergrowths".

The laths are parallelogram-shaped in cross section, and their morphology is rhombus-like (Tien 1973; Krekeler and Guggenheim 2008) (Figure 4A). Several laths of sepiolite or palygorskite can aggregate sharing faces and forming rods and bundles along the [100] direction (Figure 4B). The result of the

aggregation of the laths is the formation of irregular surfaces as a consequence of their imperfect coalescence. In this sample, the laths are 60 to 120 nm in width and 20 to 60 nm in height, which is in agreement with the (hk0)-oriented images. The TEM images reveal a high number of defects as the omission of polysomes and twins, as "The irregular surfaces of the fibers illustrate how they may coalesce imperfectly, resulting in an apparent omission of polysomes" (Krekeler and Guggenheim, 2008). Figure 4C, adapted from Krekeler and Guggenheim (2008), illustrates laths aggregation via sharing faces in a crystallographic continuity as revealed by the continuous lattice fringes. A model of laths aggregation involving the formation of rods and bundles is shown in Figure 4D. In HRTEM images of sepiolite and palygorskite natural samples rods are much more commonly found than individual laths. These rods show characteristics which could be compatible with mesocrystals as they are described by Cölfen and Antonietti (2005), since primary units can still be identified within the rods. However, to actually discriminate between mesocrystals and true new single crystals observations of cross-sections (001) are required. An example of theses cross-sections is shown in Figure 4C, where primary units are not evident and consequently these rods must be considered as true single crystals. Figure 5 shows different rod images which could correspond to either mesocrystals or new single crystals. Although in both cases the same appearance should be expected when observed parallel to the c axis, as it is schematized in Figure 4D, differences would be observed in sections parallel to (001). Therefore, the sutures that appear in the rods in Figure 5 (pointed by arrows) could be the seam zone of the primary units of mesocrystals or they could correspond to traces of the overlapping endings of crystals as it is the case in the rods shown in Figure 4C.

The disorientation produced by twists and tilts at the plane of attachment can produce defects, ranging from pure tilts to pure screw dislocations (Penn and Banfield 1998; 1999; Chun et al. 1995). Defects

247 are very frequent not only in natural sepiolite and palygorskite particles formed by oriented
248 aggregation of samples but also inside the laths. In agreement with Pen (2004), "Particles formed in
249 this manner are commonly polycrystalline particles that are composed of randomly oriented primary
250 nanocrystallites". The small size of unit crystals (laths) of sepiolite or palygorskite in the [100] and
251 [010] directions could explain the very low crystallinity found by X-ray diffraction of these samples.
252 In addition, most electron diffraction images (Figure 6) show that fibers can assume several
253 orientations around the c-axis, and these images correspond to bundles of palygorskite or sepiolite
254 fibers randomly oriented around the c-axis, revealing reflections from laths that are [110], [010], [100]
255 and [hk0] parallel to the beam. It is rarely possible to obtain the diffraction patterns of laths of only one
256 orientation as shown by Sanchez del Río et al. (2011).
257
258 After the nucleation and the oriented aggregation of the laths, the natural crystals of sepiolite and
259 palygorskite can continue growing in a much slower manner, mostly along the c-axis at the expense of
260 the diffusion of molecular scale species throughout the solution. The length of the crystals depends
261 mainly on the first stages of their nucleation and crystal growth, although in an oversaturated solution,
262 the formation of new crystals can continue and produce additional new short crystals. In contrast, the
263 slow growth of the fibers close to the equilibrium conditions can produce longer fibers. As reported by
264 Cölfen and Antonietti (2008), the formation of fiber bundle superstructures by oriented attachment is
265 especially applied to systems far from equilibrium.
266
267 According to Hartman-Perdok (1955) theory, the fibrous morphology of sepiolite and palygorskite can
268 be explained by the highly different attachment energy of their faces, which controls the morphology
269 of the particles. The crystal faces are classified depending on the number of periodic bond chain (PBC)

vectors they contain, which indicate the directions of strong bonding. The rods and bundles of sepiolite and palygorskite aggregates grow due to the incorporation of ions at energetically favorable sites. The (001) faces are the smallest faces as a consequence of their rapid growth, whereas the (hk0) faces are much larger as a result of their slower growth. The inversion of the tetrahedral sheets in the structures of sepiolite and palygorskite reduces the bond strengths at specific points in the a- and b-axis directions. The ionic bonds in the a- and b-axis directions are rather weaker than in the c-axis direction. It is necessary also take into account that in (001) faces, the tetrahedral and octahedral sheets with strong bonds, Si-O, Al-O, Mg-O and Al-OH, are broken. Nevertheless, in the (hk0) faces, Si-OH groups appear to compensate for the charge of the broken bonds in the tetrahedral sheets at the edges of the fiber, whereas octahedral sheets do not have a problem both of charge and coordination because the terminal cation in the polysomes along [001] completes its coordination sphere with two water molecules. As a consequence, the (001) faces are K faces, which leads to the growth of laths with a regular cross-section (Figure 5A, 5B, 5C and 7). The attachment energy of the (001) faces is very high and decreases greatly following the addition of atoms to complete their kinks, although immediately after of this incorporation, the energy returns to the same level as before the incorporation. However, the attachment energy of the (hk0) faces is very weak. The (hk0) faces present strong bonds by shared oxygens. These faces have to be F (flat) faces without kinks where atoms could be incorporated (Figure 7). In (110) and (010) faces, the octahedral sheet does not present broken bonds, and silanol groups complete the broken bonds in the tetrahedral sheets. Therefore, the attachment energy of the (hk0) faces is very low. The crystals have to growth in (001), generating fibrous crystal with surface tunnels, which have a very high specific surface. The only possibility of growth of the (hk0) faces is the addition of complete polysomes, which would indicate an aggregation process. This ‘weak attraction’ leads to crystallographic fusion of the two particles, eliminating the two high-energy

surfaces. The high number of defects such as twists; disorientation or tilts observed by HRTEM (Figure 4) could be evidence of their origin by aggregation or binding of minor units or polysomes.

Recently, the existence of intergrowths between sepiolite and palygorskite has been proposed based on the continuous variation of the chemical composition without a compositional lack (Suárez and García-Romero, 2011, 2013). The intermediate minerals, in regards to the chemical composition, are formed by a mixture of sepiolite and palygorskite polysomes. Thus, when a palygorskite presents sepiolite intergrown polysomes, the chemical composition corresponds to a Mg-rich palygorskite, and in the opposite extreme, a sepiolite with a portion of palygorskite polysomes appears as an Al-rich sepiolite. This can be explained by the aggregation mechanism. For solutions with a composition at the limit between the stability of the two minerals, alternative nucleation of sepiolite and palygorskite polysomes could occur in the first stage, and the polysomes of the two minerals could later aggregate to form a mixture crystal.

In oversaturated conditions, the nucleation of a large number of sepiolite and palygorskite laths must occur, and single nucleation events cannot be treated as thermodynamically independent. Nucleation must occur over an extremely short time period, in which all crystals start to nucleate at approximately the same time. The fibers of sepiolite and palygorskite that compose the natural deposits have specific textural features as a result of the thermodynamic and kinetic conditions during the nucleation process. Small changes in the conditions lead to different features among the natural deposits. These changes are responsible for the different features and properties shown by different natural deposits. The formation of short fibers could involve fast nucleation as a consequence of high supersaturation, associated with a stronger evaporative environment, whereas long fibers involve the slower growth of

316 fibers in environments with lesser supersaturation.

317

318 **Final remarks**

319

320 As has been previously explained, the growth of the crystal by addition of atoms in the [hk0] direction
321 is notably difficult when considering that the polysomatic structure of these minerals and their
322 structures determine the fibrous morphology and the high specific surface area. Accordingly, sepiolite
323 and palygorskite are perfect candidates for growth by aggregation as Cölfen and Antonietti (2005)
324 predicted, and this growth crystal mechanism is clearly indicated by the images of the present study.

325

326 The aggregation of laths explains the formation of intergrowths of sepiolite and palygorskite and,
327 at the same time, also explains the differences observed in their physical and chemical properties.
328 Accordingly, it is possible to affirm that the long of the fibers could serve to trace relative
329 changes of alkalinity-salinity in lacustrine registers containing sepiolite and palygorskite.

330

331 **Implications**

332 This is the first time the crystal growth by aggregation is referred as the main process of mineral
333 growth in natural environments. The crystal growth by aggregation is accepted as a non-classical
334 crystallization model and it has been described in recent years for synthetic materials, but this
335 work reports the growth of sepiolite-palygorskite minerals by aggregation, which involves
336 oriented aggregation of nanoparticles and mesocrystals formation.

337

338 There are remarkable HRTEM images of sepiolite-palygorskite crystals illustrating the steps of
339 growth of different faces with highly different attachment energy, which controls the
340 morphology of fibrous particles.

341

342 In addition, this work provides information concerning to the precipitation of these minerals in
343 aquatic environments, which contributes to the knowledge of the physico-chemical conditions
344 existent during the formation of numerous deposits of both minerals, some of which have high
345 economic importance.

346

347 **Acknowledgments**

348

349 The financial support of the MINECO (CGL2012-35475) is acknowledged. We are also very
350 grateful to Drs. Viedma and Fernández Diaz for their help.

351

352 **References cited**

353

354 Alivisatos, A. P. (2000) Biomineralization - Naturally aligned nanocrystals. Science 289, (5480), 736-
355 737.

356

357 Álvarez, A. (1984) Sepiolite properties and uses, In: Playgorskite-Sepiolite: Occurrences, genesis and
358 Uses. A. Singer and E. Galán E. Editors. Elsevier, New York, 253-287.

359

Álvarez, A.; Santarén, J.; Esteban-Cubillo, A. and Aparicio, P. (2011) Current industrial applications of palygorskite and sepiolite. In: In: Advances in the crystal chemistry of sepiolite and palygorskite. Developments in Palygorskite-Sepiolite Research. Galán E. and Singer A. edit. Chapter 12. Developments in Clay Science, Vol. 3, Elsevier. 281-298.

Banfield, J. F. Welch, S. A.; Zhang, H. Z.; Ebert, T. T. and. Penn, R. L. (2000) Aggregation-based crystal growth and microstructure development in natural iron oxyhydroxide biomineralization products. Science, 289, 751-754

Billotti, E., Fischer, H.R., Peijs, T. (2008) Polymer nanocomposites based on needle-like sepiolite clays: effect of functionalized polymers on the dispersion of nanofiller, crystallinity, and mechanical properties. Journal Applied Polymer Science. 107, 1116–1123.

Carretero, M.I. (2002) Clay Minerals and their beneficial effects upon human health.A review.Applied Clay Science, 21, 155–163.

Carretero, M.I., Gomes, C.S.F., Tateo, F. (2006) Clays and human health. In: Bergaya, F. et al. (Ed.), Handbook of Clay Science. Developments in Clay Science. Elsevier, Amsterdam, pp. 717–741.

Cho, K.S.; Talapin, D.V.; Gaschler, W. and Murray, C. B. (2005) Designing PbSe Nanowires and Nanorings through Oriented Attachment of Nanoparticles. Journal America Chemical Society, 127, 7140-7147.

383 Chryssikos, G. D.; Gionis, V.; Kacandes, G.H.; Statopoulou, E. T.; Suárez, M.: García-Romero, E. and
384 Sánchez del Río, M. (2009) Octahedral cation distribution in palygorskite. American Mineralogist, 94,
385 200-203.
386
387 Chun, C.M. Navrostsky, A. and Aksay, I.A. (1995) Aggregation growth of nanometer-size $BaTiO_3$
388 Particles. In: Proc. Microscopy and Microanalysis. Bailey, G. W, Ellisman, M.H, Hennigar, R.A. and
389 Zluzec, N.J. editors. Jones & Beuel.188-189.
390
391 Cölfen H. and Antonietti, M. (2005) Mesocrystals: Inorganic superstructures made by highly parallel
392 crystallization and controlled alignment. Angewandte Chemie. 44, 5576 – 5591.
393
394 Cölfen, H. and Antonietti, M. (2008) Mesocrystals and Nonclassical Crystallization. John Wiley & Sons
395 Ltd, T. England, 276 pp.
396
397 Cornejo, J., (1990) Las arcillas en formulaciones farmacéuticas. In: Galán, E., Ortega, M. (Eds.),
398 Conferencias de la IX y X Reuniones de la Sociedad Española de Arcillas, SEA (Madrid), pp. 51–68.
399
400 Eberl, D. D.; Blum, A.E. and Serravezza, M. (2011) Anatomy of a metabentonite: Nucleation and growth
401 of illite crystals and their coalescence into mixed-layer illite/smectite. American Mineralogist, 96, 586-
402 593.
403
404 García-Romero, E. and Suárez, M. (2010) On the chemical composition of sepiolite and palygorskite.
405 Clays and Clay Minerals, 58, 1, 1–20.

García-Romero, E. and Suárez, M. (2012) Sepiolita-Palygorskita: un ejemplo de cristalización no clásica. Macla, 16, 96-97.

García-Romero, E. and Suárez, M. (2013-a) Oriented aggregation as crystal growth mechanism: the sepiolite-palygorskite polysomatic series. 2nd International Conference Clays, Clay Minerals and Layered Materials – CMLM2013.St Petersburg. Book of abstracts, 37.

García-Romero, E. and Suárez, M. (2013-b) Sepiolite-palygorskite: Textural study and genetic considerations. Applied Clay Science, 86, 129-144.

García-Romero, E.; Suárez, M. and Bustillo, M.A. (2004) Characteristics of a Mg-palygorskite in Miocene rocks, Madrid Basin (Spain). Clays and Clay Minerals, 52, 4, 484–494,

García-Romero, E.; Suárez, M.; Santarén, J. and Álvarez, A. (2007) Crystallochemical characterization of the palygorskite and sepiolite from the Allou Kagne deposit. Senegal. Clays and Clay Minerals, 6, 606-617.

Gassmann, O.; Beder, R. B.; Putnis, A. and Löbmann, P. (2003) Biomimetic control of crystal assembly by growth in an organic hydrogel network. American Mineralogist, 88, 647-652.

Gibbs, J. W. 1948. Thermodynamics, Collected works Vol. I; Yale University Press: New Haven, CT,

429 Hartman, P. and Perdok, W.G. (1955) On the relations between structure and morphology of crystals.
430 Acta Crystallographica, 8, 49–52.
431
432 Jones B. F, and Galán, E. (1991) Sepiolite and palygorskite. In: Hidrousphyllosilicates (exclusive of
433 micas). S. W. Bailey Editor. Reviews in Mineralogy.Vol. 19. Mineralogical Society of America.631-
434 674
435
436 Krekeler M.P.S. and Guggenheim S. (2008) Defects in microstructure in palygorskite-sepiolite minerals:
437 A transmission electron microscopy (TEM) study. Applied Clay Science, 39, 1, 98-105.
438
439 Leguey, S., Cuevas, J., Ruiz, A.I. and Ruiz León, D. (2010). The role of biomineralization in the origin of
440 sepiolite and dolomite. American Journal of Science. 310, 165–193.
441
442 López-Galindo, A., Viseras, C. (2004) Pharmaceutical and cosmetic applications of clays. In: Wypych, F.,
443 Satyanarayana, K.G. (Eds.), Clay Surfaces: Fundamentals and Applications. Elsevier, Amsterdam, pp.
444 267–289.
445
446 López-Galindo, A., Viseras, C.; Aguzzi, C. and Cerezo, P. (2011) Pharmaceutical and cosmetic uses of
447 fibrous clays. Developments in Palygorskite-Sepiolite Research. Galán E. and Singer A. edit. Chapter
448 13.Developments in Clay Science, Vol. 3, Elsevier.299-324.
449
450 Martín Vivaldi J. L. and Robertson, R. H. S. (1971) Palygorskite and Sepiolite (The Hormites), in
451 Reprinted from the Electron-Optical Investigation of Clays. Gard, J. A. ed. The mineralogical Society,

452 41, 255-257.

453

454 Meunier, (2005) Clays. Springer. Berlin, 472 pp.

455

456 Murphy, C. J. and Jana, N. R. (2002) Controlling the aspect ratio of inorganic nanorods and nanowires.
457 Advanced Materials. 14, 80–82.

458

459 Murray, H. H. (1999) Applied clay mineralogy today and tomorrow. Clay Minerals. 34, 1, 39-49.

460

461 Nespolo, M. (2001)Perturbative theory of mica polytypism. Role of the M2 layer in the formation of
462 inhomogeneous polytypes. Clays and Clay Minerals. 40, 1-23

463

464 Ostwald, W. (1896) Lehrbuch der Allgemeinen Chemie, Vol. 2, Part 1; Leipzig, Germany.

465

466 Penn, R. L. 2004. Kinetics of Oriented Aggregation. Journal Physico Chemical Bouletin, 108, 12707-
467 12712.

468

469 Penn, R. L. (2004) Kinetics of Oriented Aggregation. Journal Physic Chemistry B, 108, 12707-12712.

470

471 Penn, R.L. and Banfield, J.F. (1998) Imperfect oriented attachment: a mechanism for dislocation
472 generation in defect-free nanocrystals. Science, 281, 969-971.

473

474 Penn, R. L., and Banfield, J. F. (1999) Morphology development and crystal growth in nanocrystalline

475 aggregates under hydrothermal conditions: Insights from titania. Geochimica et Cosmochimica Acta
476 63, 10, 1549-1557.
477
478 Ruiz-Hitzky, E., Aranda, P., Serratosa, J.M., (2004) Organic/Polymeric Interactions with Clays. In:
479 Auerbach, S.M., Carrado, K.A., Dutta, P.K. (Eds.), Handbook of Layered Materials. Marcel Dekker,
480 New York, pp. 91–154 (Chapter 3).
481
482 Ruiz-Hitzky, E.; Aranda, P.; Álvarez, A.; Santarén, J. and Esteban-Cubillo, A. (2011) Advanced
483 Materials and New applications of sepiolite and palygorskite In: Advances in the crystal chemistry of
484 sepiolite and palygorskite. Developments in Palygorskite-Sepiolite Research. Galán E. and Singer A.
485 edit. Chapter 17. Developments in Clay Science, Vol. 3, Elsevier. 293-452.
486
487 Ruiz-Hitzky, E., Van Meerbeek, A. (2006) Development in clay science. In: Bergaya, F., Theng, B.K.G.,
488 Lagaly, G. (Eds.), Clay Mineral- and Organoclay–Polymer nanocomposite. Handbook of Clay Science.
489 Elsevier, Amsterdam, pp. 583–621 (Chapter 10.3).
490
491 Sánchez del Río, M.; Doménech, A.; Doménech-Carbo, M.T.; Vázquez de AgredosPascual, M.L.;
492 Suárez, M.; and García-Romero. E. (2011) The Maya Blue Pigment. In: Advances in the crystal
493 chemistry of sepiolite and palygorskite. Developments in Palygorskite-Sepiolite Research. Galán E.
494 and Singer A. edit. Chapter 17. Developments in Clay Science, Vol. 3, Elsevier. 293-452.
495
496 Sánchez del Río M., Suárez, M. and García-Romero, E. (2009) The occurrence of palygorskite in the
497 Yucatán peninsula: Ethno-historic and archaeological contexts. Archaeometry, 51, 2, 214-230.

498

499 Sánchez del Río, M. García-Romero, E. Suárez, M.; da Silva, I.; Fuentes-Montero, L. and Martínez-
500 Criado., G. (2011) Variability in sepiolite: Diffraction studies. American Mineralogist, 96, 1443–1454,

501

502 Singer, A. (1981) The texture of palygorskite from The Rift Valley, Southern Israel. Clay Minerals, 16,
503 415-419.

504

505 Soliman, M.F and El Goresi, A. (2012) Framboidal and idiomorphic pyrite in the upper Maastrichtian
506 sedimentary rocks at Gabal Oweina, Nile Valley, Egypt: Formation processes, oxidation products and
507 genetic implications to the origin of framboidal pyrite. Geochimica et Cosmochimica Acta, 90, 195–
508 220.

509

510 Stathopoulou, E.T.; Suárez, M.; García-Romero, E.; Sánchez del Río, M.; Kacandes, G.H.; Gionis, V. and
511 Chryssikos, G.D. (2011) Trioctahedral entities in palygorskite: Near-infrared evidence for sepiolite-
512 palygorskite polysomatism, European Journal of Mineralogy, 23, 4.

513

514 Suárez M. and García-Romero E. (2006) FTIR spectroscopic study of palygorskite: Influence of the
515 composition of the octahedral sheet. Applied Clay Science, 31, 154-163.

516

517 Suárez, M. and García-Romero, E. (2006) Macroscopic palygorskite form Lisbom Volcanic Complex.
518 European Journal of Mineralogy, 18, 119-126

519

520 Suárez, M. and García-Romero, E. (2011) Advances in the crystal Chemistry of Sepiolite and

521 Palygorskite. Ch:2 In: Developments in Palygorskite-Sepiolite Research. A new outlook on these
522 nanomaterials. Ed. E. Galán and A. Singer. Elsevier, 500 pp.
523
524 Suárez, M. and García-Romero, E. (2012) Variability of the surface properties of sepiolite.Applied Clay
525 Science, 67, 72-82.
526
527 Suárez, M. and García-Romero, E. (2013) Sepiolite–Palygorskite: A continuous polysomatic series. Clays
528 and Clay Minerals. 61, 461-472,
529
530 Suárez, M.; García-Romero, E.; Sánchez del Río, M.; Martinetto, P. and Dooryhée, E. (2007) The effect
531 of the octahedral cations on the dimensions of the palygorskite cell. Clay Minerals. 42, 287-297.
532
533 Suárez, M., Robert, M., Elsass, F. and Martín Pozas, J.M. (1994) Evidence of a precursor in the
534 neoformation of palygorskite- New data by analytical electron microscopy. Clay Minerals, 29, 255
535 264.
536
537 Tien, P. L. 1973. Palygorskite from Warren Quearry Enderby, Leicestershire, England, Clay Minerals, 10,
538 27-34.
539
540 Yuwono, V.M; Burrows, N.D; Soltis J.A; and Penn, R.L (2010) Oriented Aggregation: Formation and
541 Transformation of Mesocrystal Intermediates Revealed. Journal of the American Chemical Society,
542 ASAP publication date 29 January 2010.
543

544

545 **Figure captions**

546

547 Figure 1.Structural schemes of palygorskite and sepiolite (adapted from Suárez and García-Romero
548 2011). a) and b) Tetrahedral sheets of palygorskite and sepiolite, respectively, projected on (100),
549 black and gray mean tetrahedrons with apical oxygens pointing in opposite directions. c) and d)
550 Tetrahedral sheets of palygorskite
551 andsepiolite, respectively, projected on (001).

552

553 Figure 2. TEM Images of sepiolite and palygorskite. A) Palygorskite prismatic crystals (laths)
554 elongated along the [001] direction (Palygorskaya, Russia). B) Sepiolite prismatic crystals (laths)
555 elongated along the [001] direction and aggregated parallel to the c-axis, forming rods (Grant County,
556 USA). C) End of bundles of palygorskiteformed by laths grouped more or less parallel to the c-axis
557 (Attapulgus, France). D) Bundle of sepiolite. (Vallecas, Spain). E) Bundle of palygorskiteformed by
558 laths grouped more or less parallel to the c-axis without sharing faces or edges (Attapulgus, France).
559 Note than the laths are shorter than the bundle. F)The grouping of palygorskite rods forms bundles
560 (Pics Crossing, Australia).

561

562 Figure 3.MEB-FEG images of sepiolite and palygorskite. A and B) Crystals (laths) elongated along the
563 [001] direction aggregatedsharing faces, forming rods. C and E) Detail of D. C) Laths (detail of D). E)
564 Laths aggregated forming rods (detail of D). A) Sepiolite, Namibia. B) Palygorskite, Boa Vista, Brazil.
565 C, D and E) Palygorskite, Okehampton (UK).

566

Figure 4. HRTEM images of cross-section of fibers. A) Cross-section of a lath showing a rhombus-like morphology (Sepiolite, Norway). B) Cross-section of bundle made by rods revealing the irregular surfaces that are a consequence of their imperfect coalescence (Sepiolite, Norway). C) Cross-section of sepiolite fibers laths aggregated by mean of sharing faces in a crystallographic continuity forming new single crystals (Image from Krekeler and Guggenheim (2008)). D) Scheme of polysome, lath, rod and bundle. The bundle is formed by three rods in more or less parallel arrangement. Each rod is formed by aggregation of laths in crystallographic continuity. One rod is a new single crystal while another is a mesocrystal.

Figure 5. HRTEM rods images. Sepiolite (Gran County, U.S.A.). K (kinked faces). F (flat faces). Arrows point to the sutures into rods.

Figure 6. A) SAED corresponding to bundles in the box in image. B) Image of palygorskite (Serrata de Nijar, Spain). C) SAED corresponding to bundle in the box in image. D) Palygorskite (Boa Bista, Brassil). Note that SAED corresponds to fibers that can assume several orientations

Figure 7. HRTEM images of the end of laths of sepiolite (Norway) showing F (flat faces), K (kinked faces) and steps of growth.

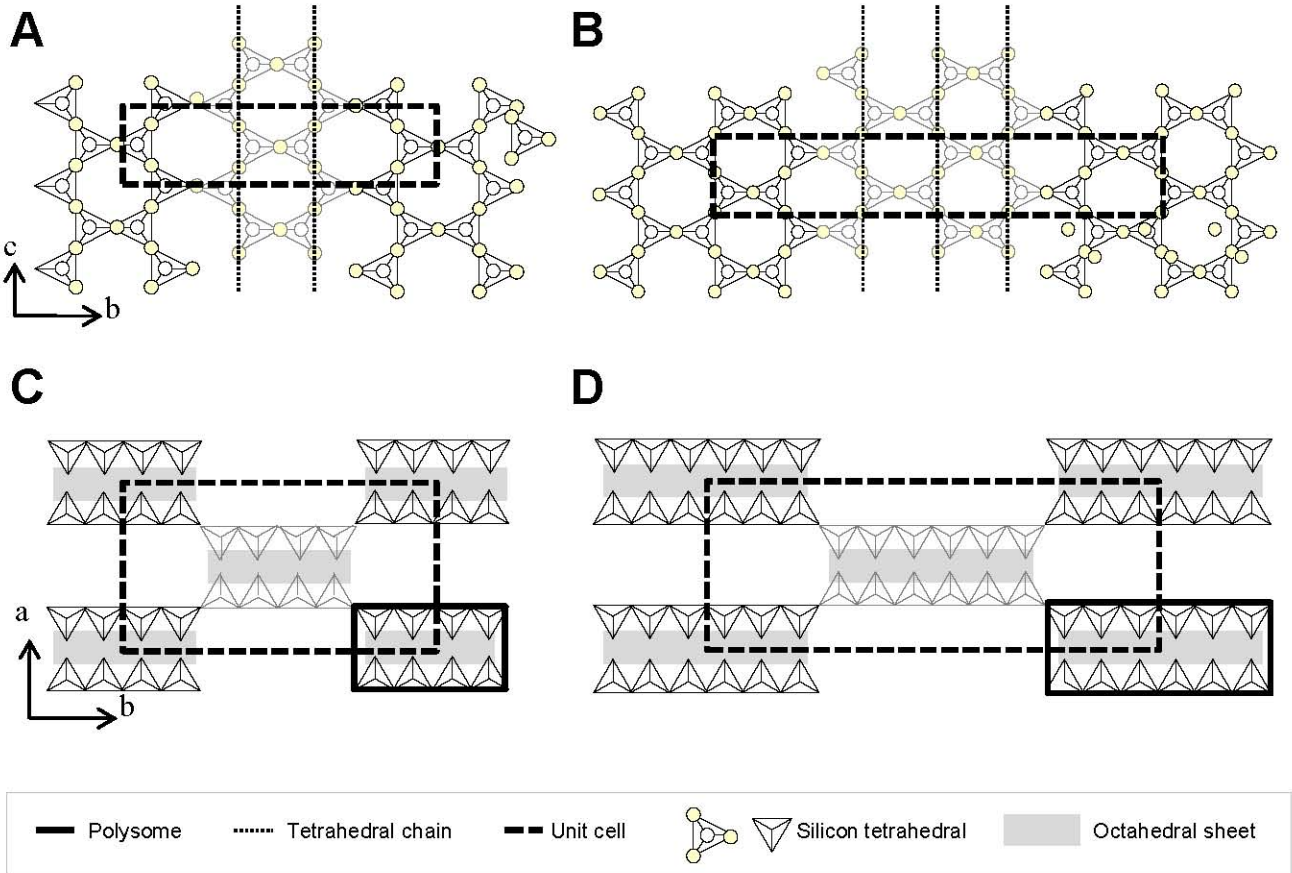
A
B
C
D
c
b
a
b
Polysome
Tetrahedral chain
Unit cell
Silicon tetrahedral
Octahedral sheet

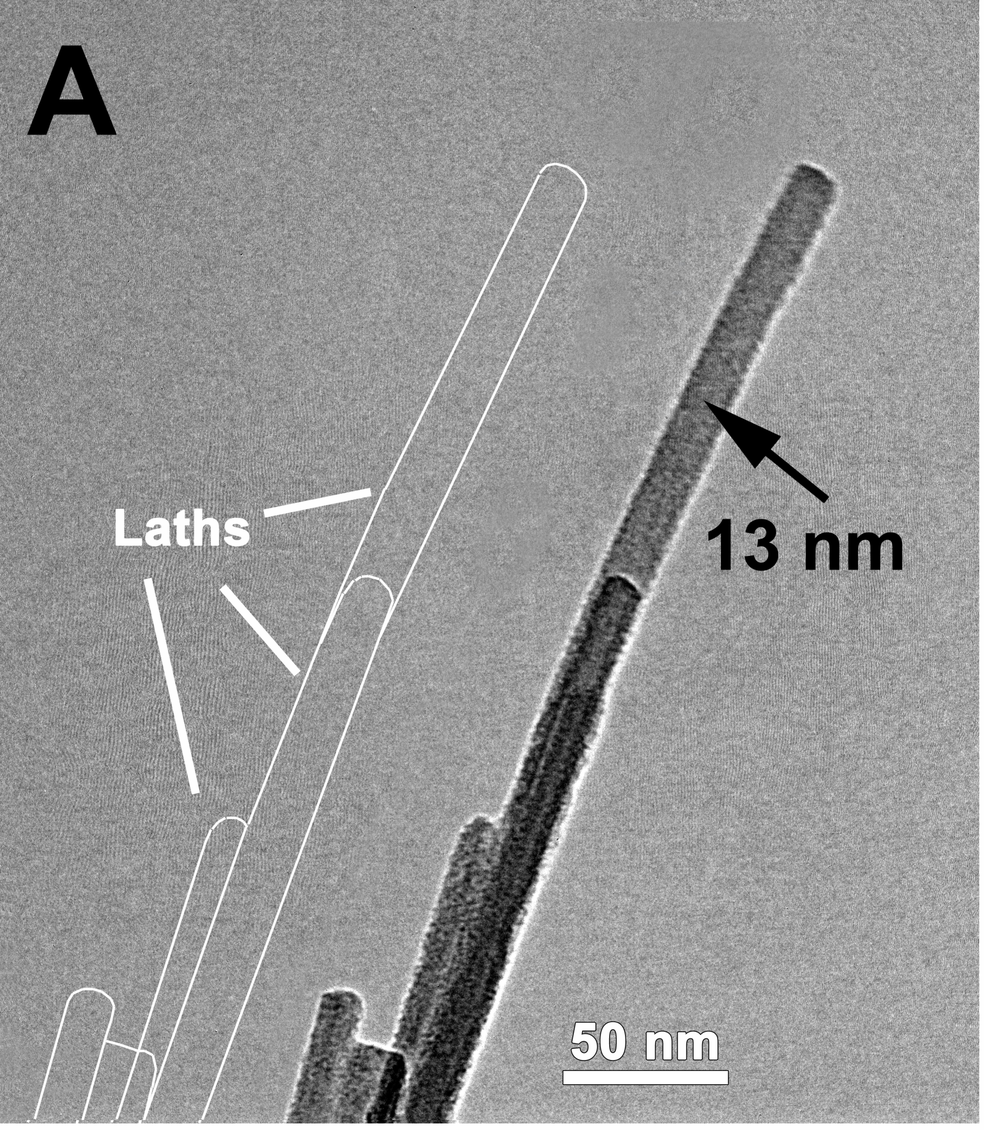
A
Laths
13 nm
50 nm

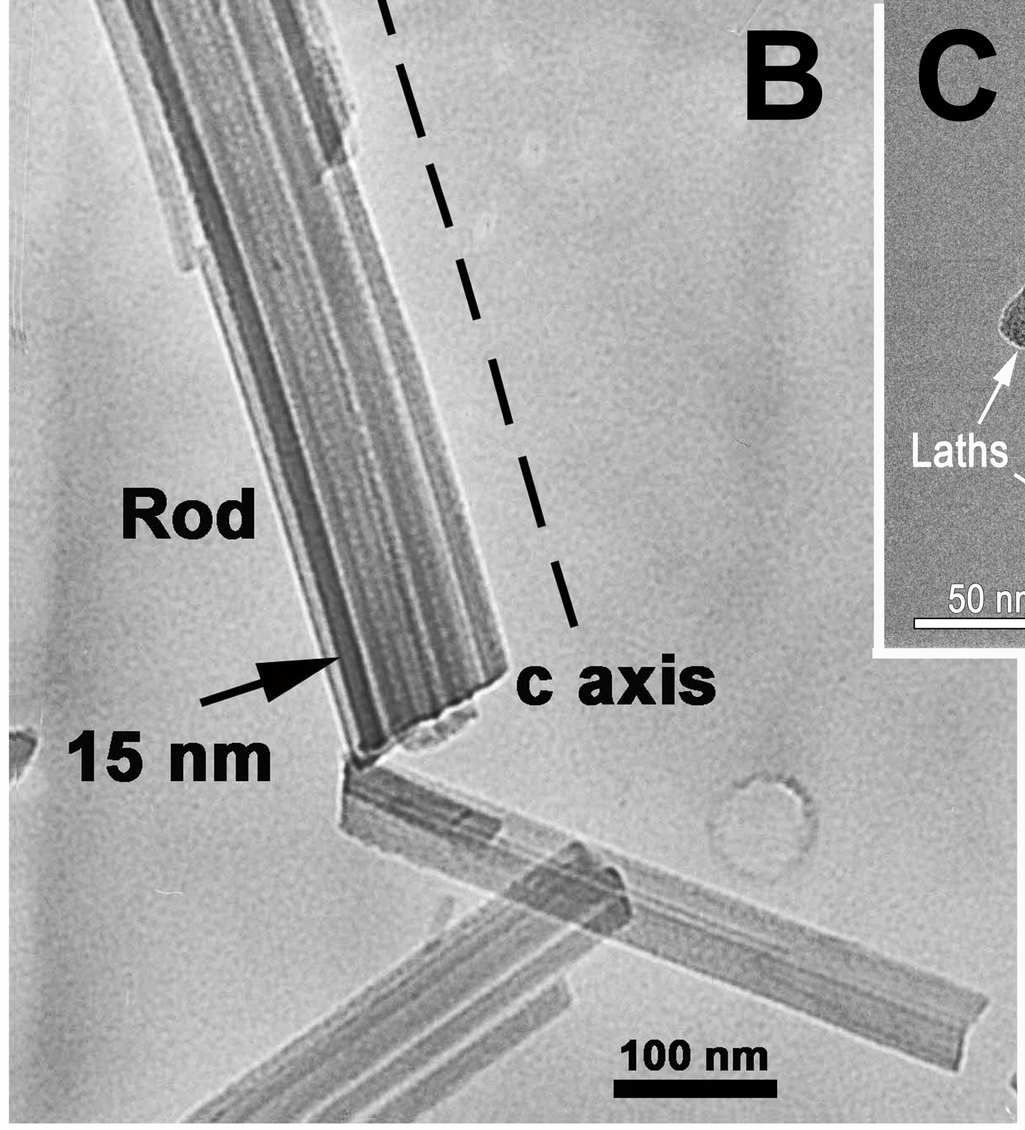
B
Rod
15 nm
c axis
100 nm

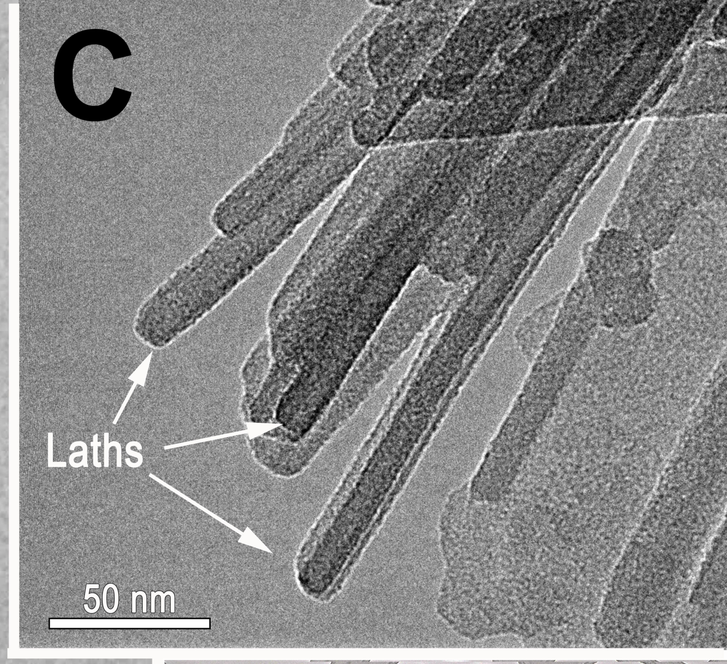
C
Laths
50 nm

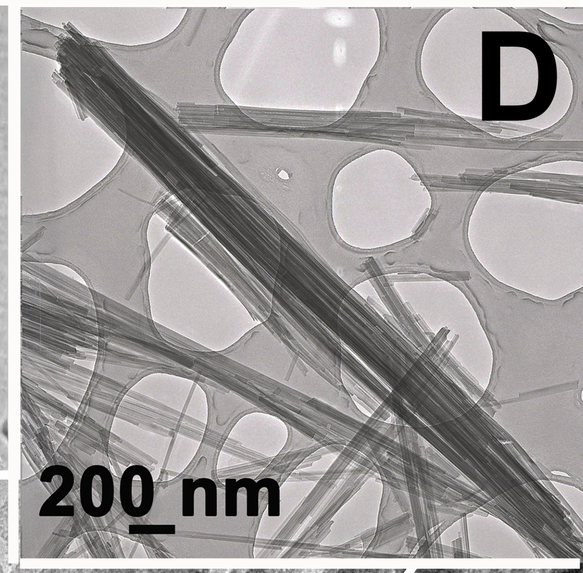
D
200 nm

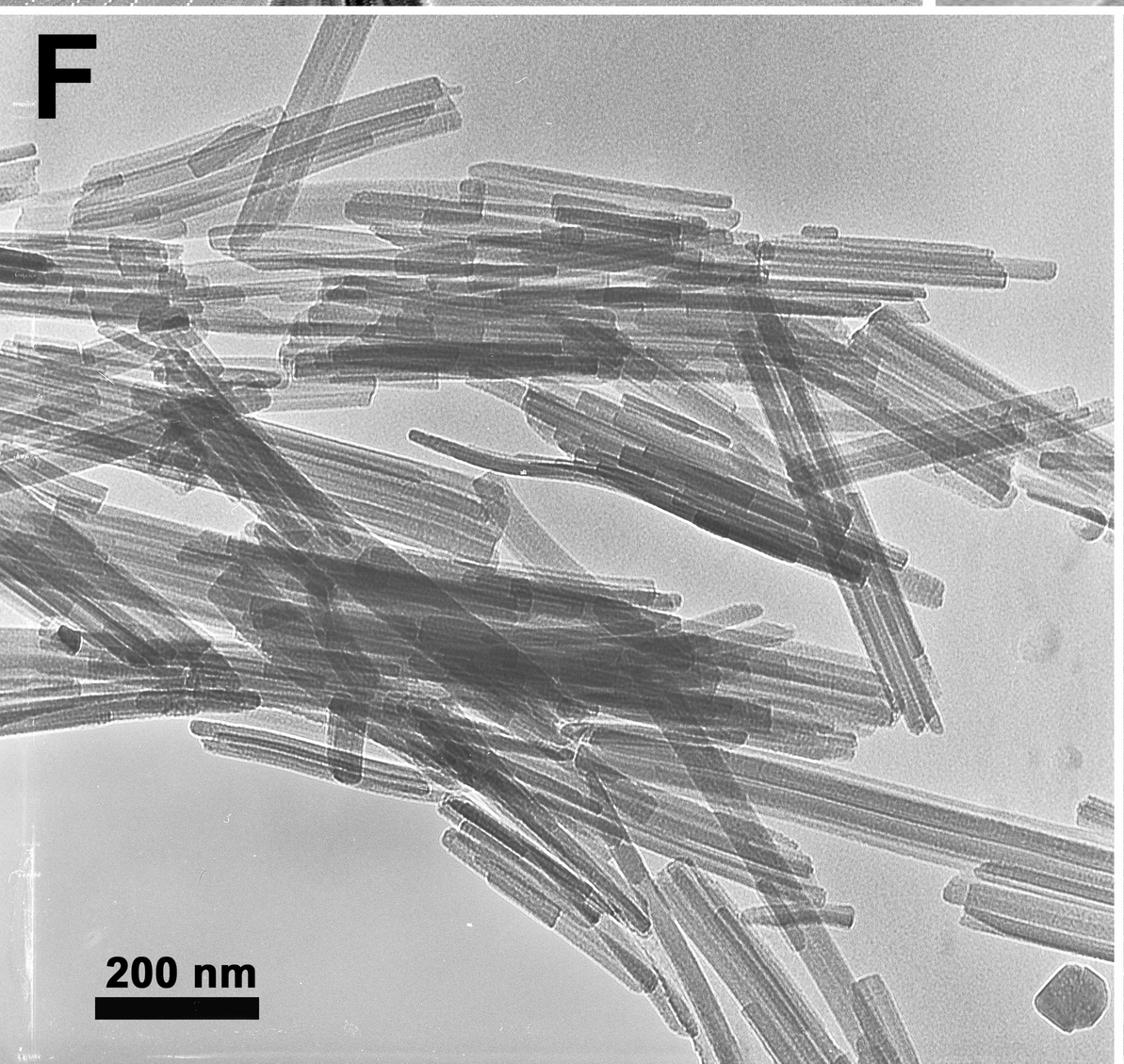
F
200 nm

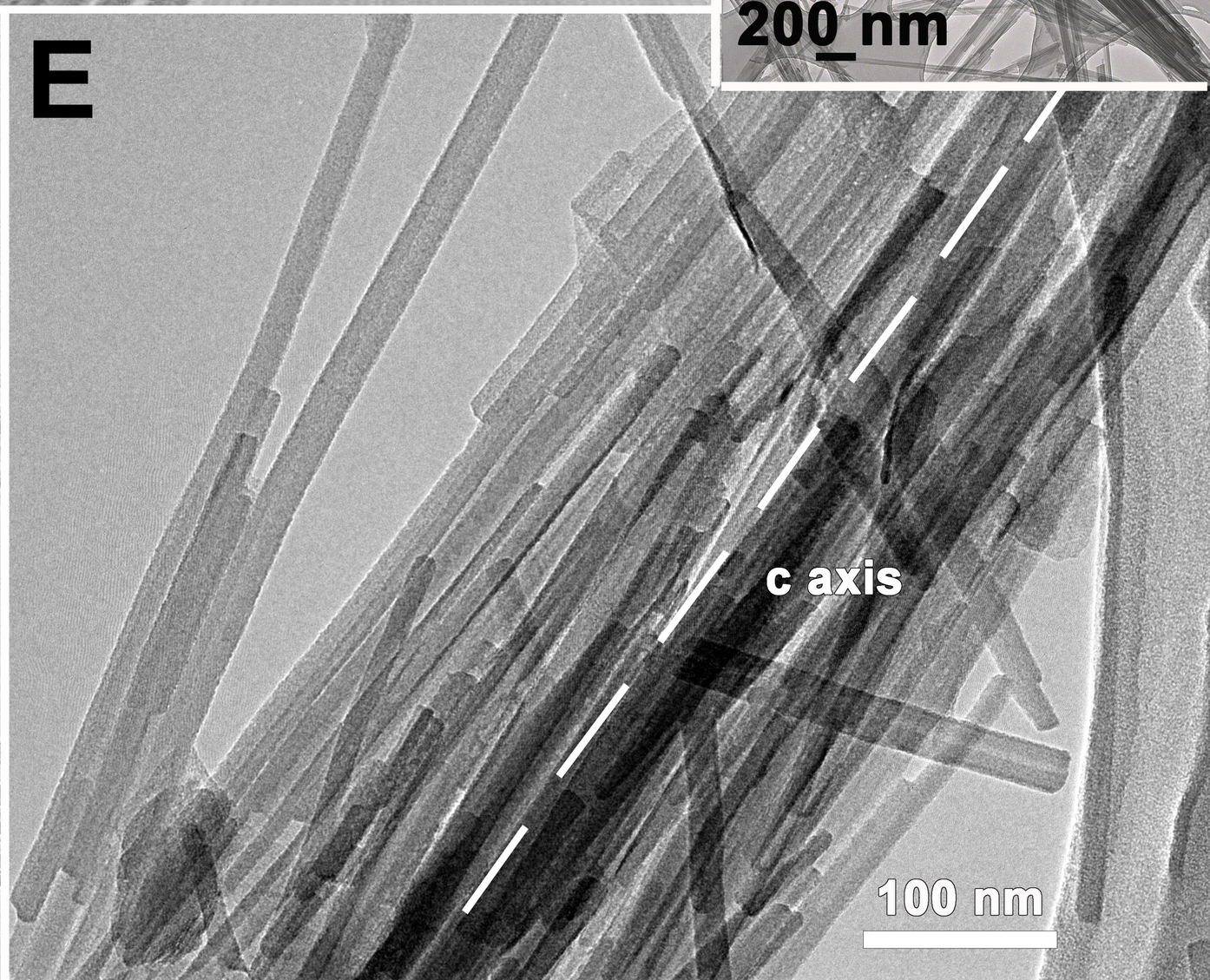
E
c axis
100 nm

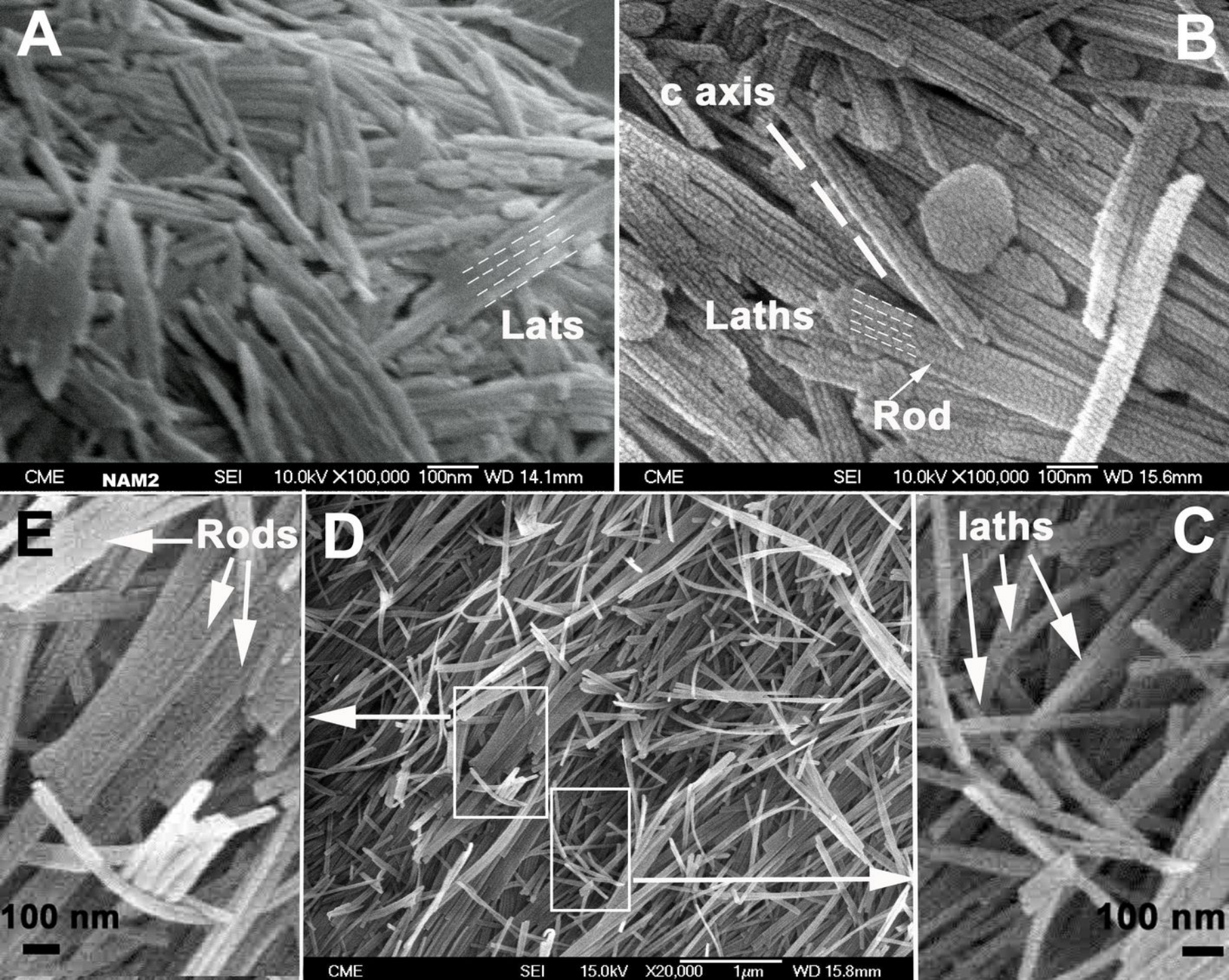
A
Lats
CME NAM2 SEI 10.0kV X100,000 100nm WD 14.1mm
B
c axis
Laths
Rod
CME SEI 10.0kV X100,000 100nm WD 15.6mm
E
Rods
100 nm
D
CME SEI 15.0kV X20,000 1μm WD 15.8mm
C
laths
100 nm

A

50 nm

B

Rod

Rod

Rod

100 nm

C

(001)

(010)

O

10 nm

D

Rod
Single crystal

Rod
Mesocrystal

Lath

Polysome

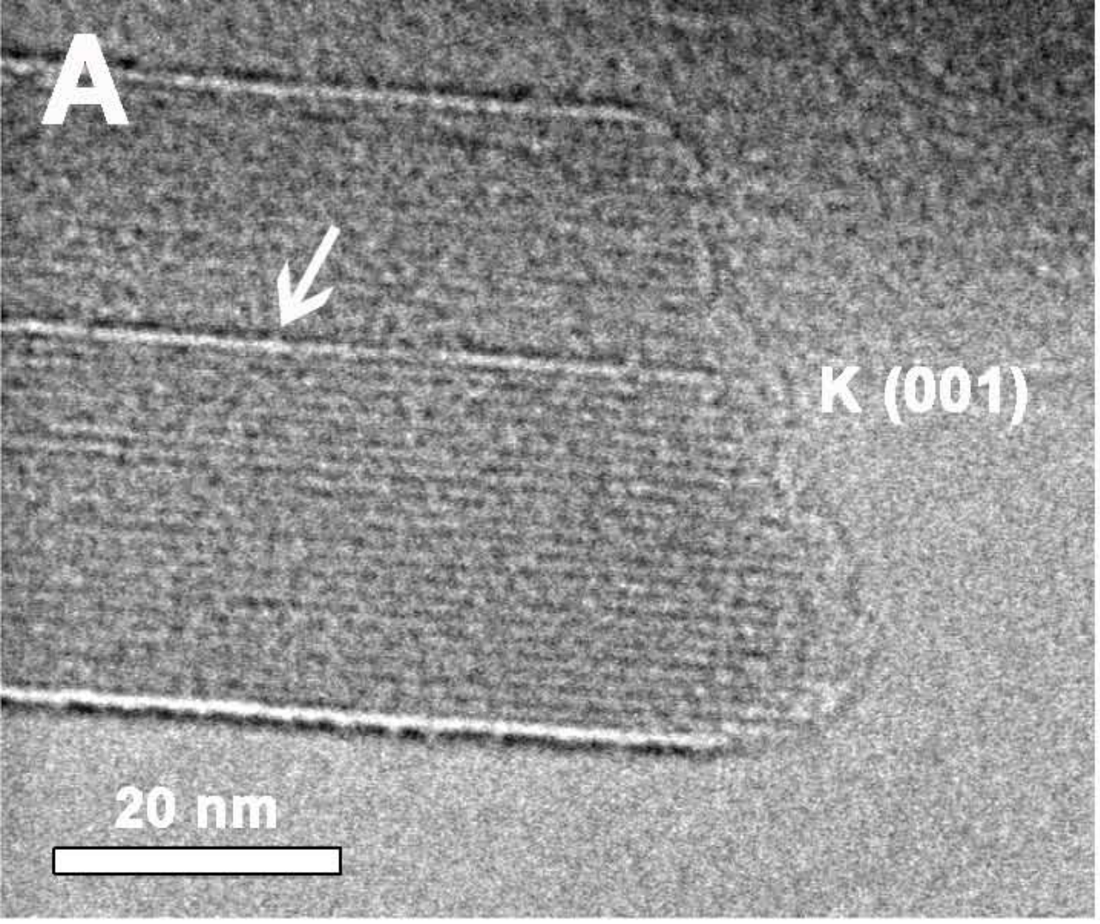
A
K (001)
20 nm

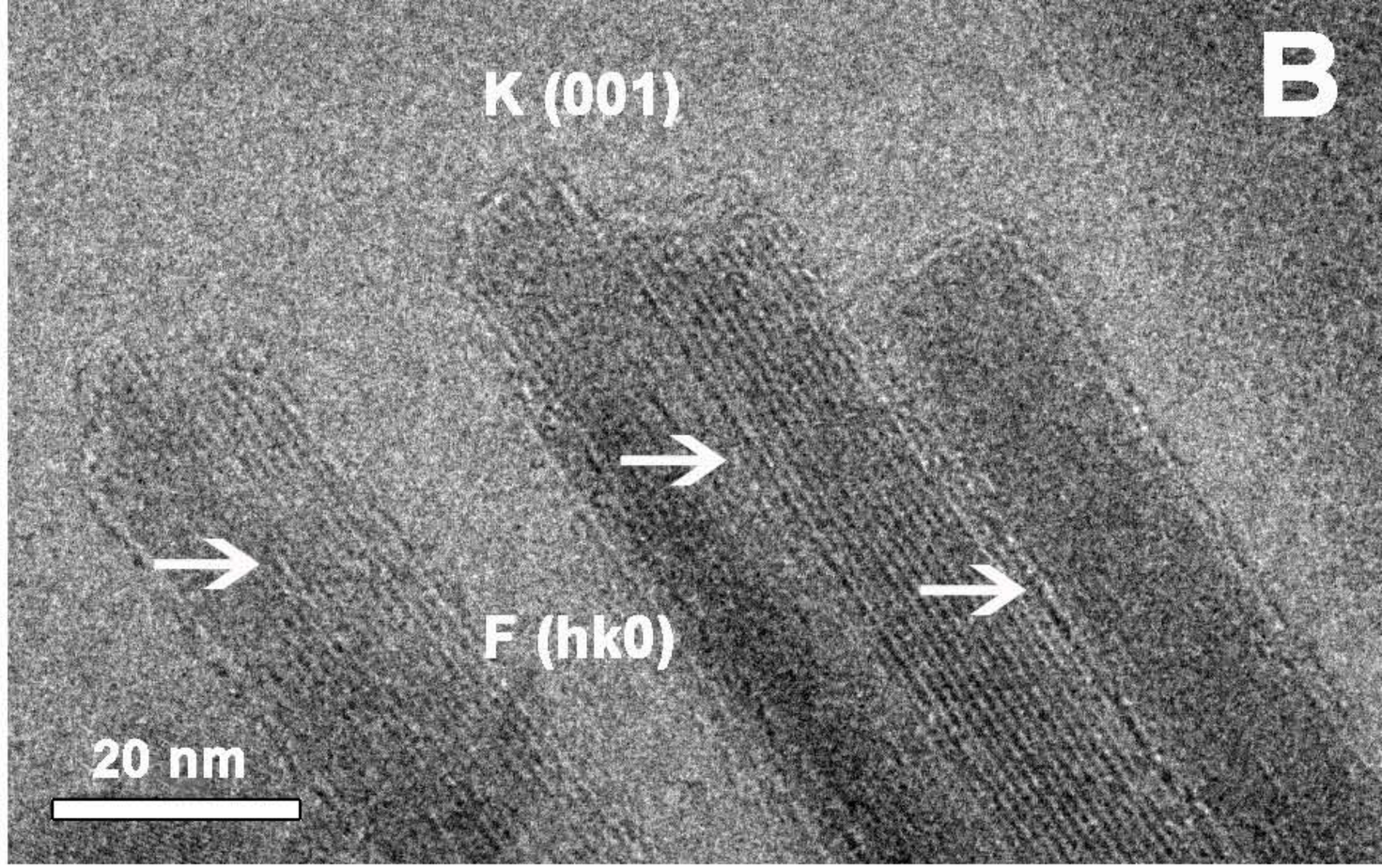
K (001)
B
F (hk0)
20 nm

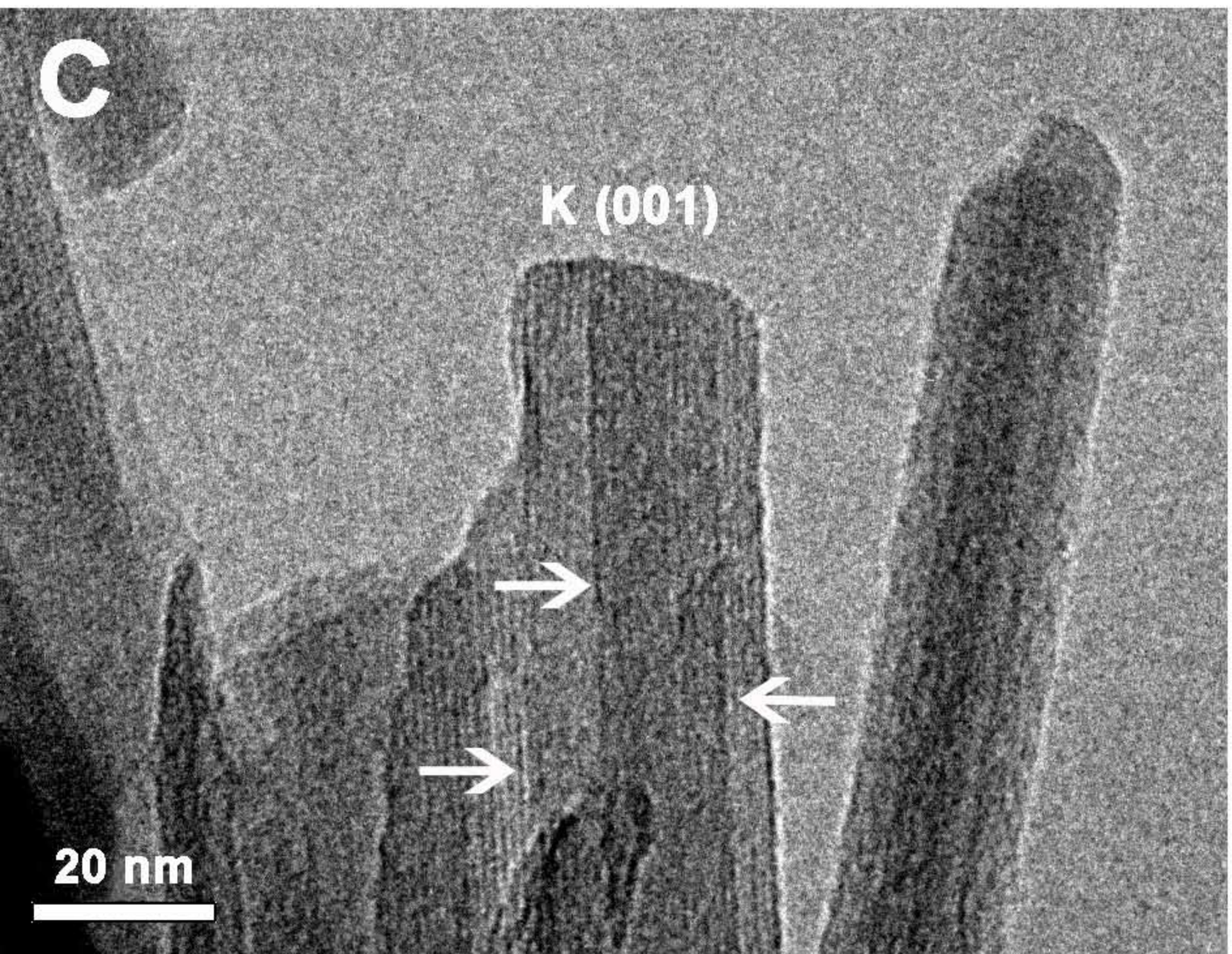
C
K (001)
20 nm

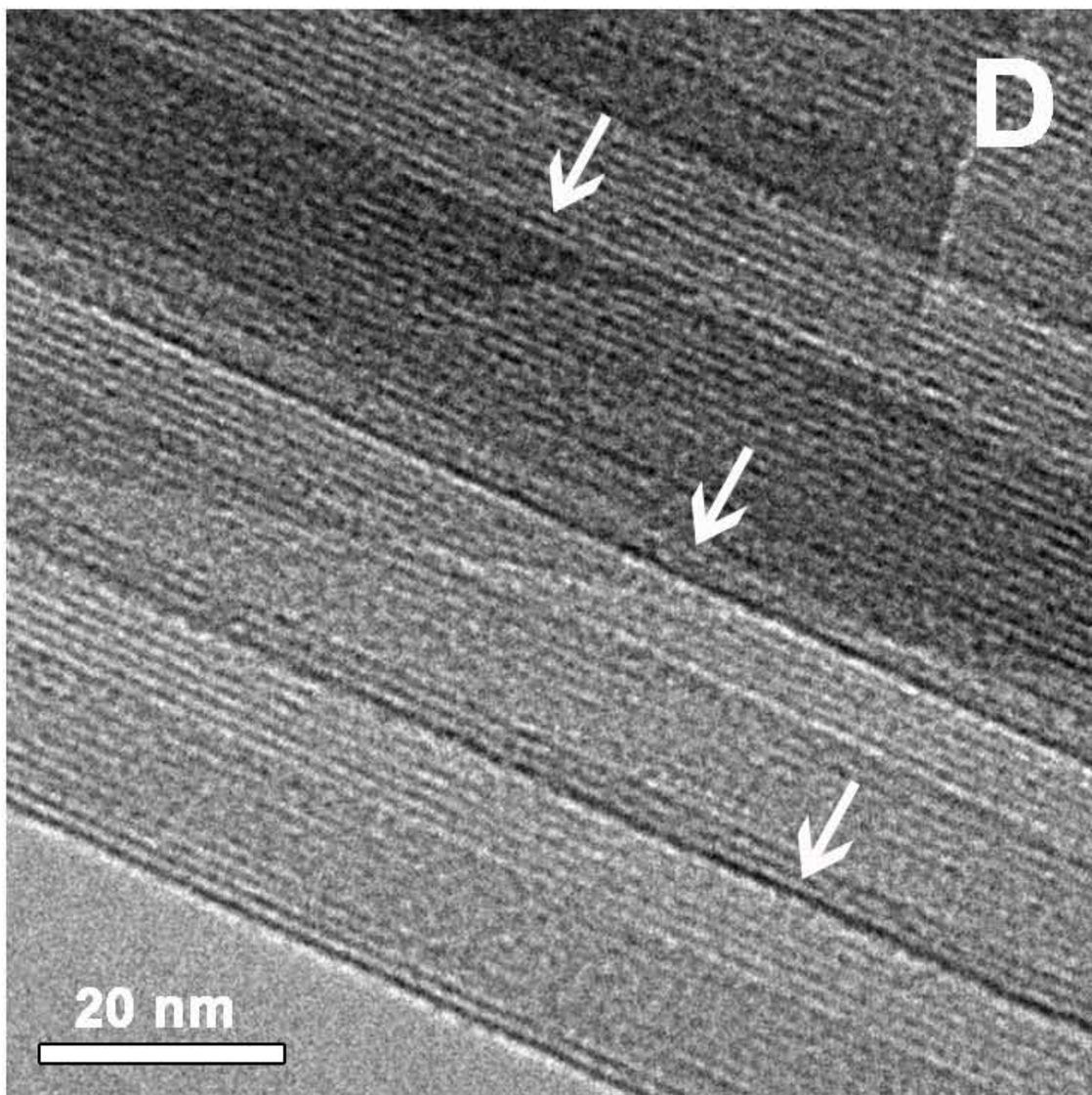
D
20 nm

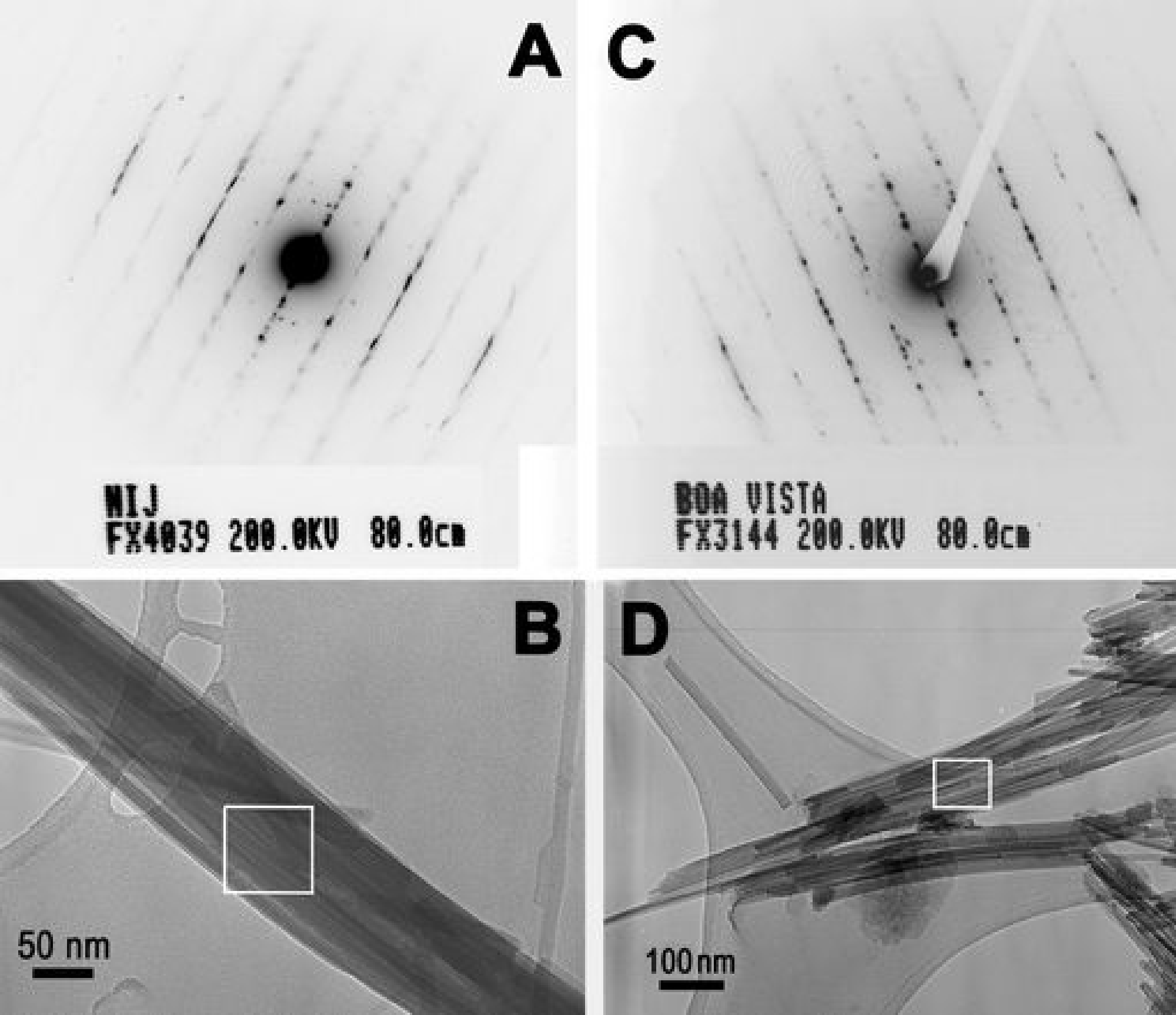
A
C
NIJ
FX4039 200.0KV 80.0cm
BOA VISTA
FX3144 200.0KV 80.0cm
B
D
50 nm
100 nm

Growth Steps

d = 12 Å

F(hk0)

K(001)

20 nm

K(001)

20 nm